

EXTENSION OF  $R$  MATRIX THEORY\*

I. ROTTER

Max-Planck-Institut für Physik komplexer Systeme  
D-01187 Dresden, Germany*(Received February 10, 2004)*

The unified description of nuclear structure and nuclear reaction aspects allows to calculate, in a consistent manner, the spectroscopic values of the nucleus that is treated as an open quantum system. The  $E_k$ ,  $\Gamma_k$  follow from the energy dependent eigenvalues  $\tilde{E}_k - i/2 \tilde{\Gamma}_k$  of the effective Hamiltonian  $\mathcal{H}$  describing the nucleus embedded in the continuum of decay channels. The coupling matrix elements  $\tilde{\gamma}_{kc}$  between the resonance states  $k$  and the decay channels  $c$  are calculated by means of the eigenfunctions of  $\mathcal{H}$ . They are complex and energy dependent. The  $S$  matrix contains the  $\tilde{E}_k$ ,  $\tilde{\Gamma}_k$  and  $\tilde{\gamma}_{kc}$ . The  $R$  matrix can therefore be generalized in a natural manner by replacing the standard spectroscopic parameters  $E_k^R$ ,  $\Gamma_k^R$  and  $\gamma_{kc}^R$  by the energy dependent functions  $\tilde{E}_k$ ,  $\tilde{\Gamma}_k$  and  $\tilde{\gamma}_{kc}$ . This new version of  $R$  matrix allows the extraction of spectroscopic information also from nuclear reactions near decay thresholds and in the regime of high level density where narrow resonances appear together with broad ones. Surface effects play a role similar as in the standard theory.

PACS numbers: 21.30.-x, 24.30.-v, 32.80.Bx, 66.35.+a

**1. Introduction**

In standard nuclear reaction calculations, the nuclear structure aspects are implemented into the  $S$  matrix by using the  $R$  matrix formalism. According to the standard work [1] on  $R$  matrix theory of nuclear reactions, its essential feature is the occurrence of a complete set of many-particle states defined in a volume of nuclear size by the imposition of some fixed boundary condition on the surface of this volume. That means, the  $R$  matrix theory specifies the form of the wave functions on the surface of the nucleus. Since the  $S$  matrix specifies their form at infinity, a connection between the two matrices has to be established by joining these regions. The process of joining introduces into the  $R$  matrix theory reference to external wave functions [1].

---

\* Presented at the XXVIII Mazurian Lakes School of Physics, Krzyże, Poland, August 31–September 7, 2003.

The standard studies for decaying states are performed in the following manner. First, the Hermitian Hamiltonian  $H = H_0 + V$  of the nucleus inside a volume of nuclear size with appropriate shape of the surface is diagonalized and its (real) eigenvalues and eigenfunctions are identified with the energies  $E_k^0$  and wave functions  $\Phi_k^0$  of the different discrete states  $k$  of the nucleus. In a second step, the spectroscopic factors  $S_k^c$  are calculated which transform the wave functions into their channel representation,  $\Phi_k^A = \Phi_k^{(A-a)} \otimes \Phi_k^a$ , where  $c \equiv (A - a) \oplus a$  is the channel. The link between the interior of the nucleus and its environment (continuum of decay channels) is then established by the penetration factor  $P_c$  that is calculated on the nuclear surface. It translates  $(\Phi_k^a)_{\text{bound}}$  to  $(\Phi_k^a)_{\text{unbound}}$ . Using these values, the partial widths can be calculated:  $|\gamma_{kc}^R|^2 = S_k^c \otimes P_c$ . Finally, by summing up these values for all open decay channels  $c$ , the decay widths are obtained:  $\Gamma_k^R = \sum_c |\gamma_{kc}^R|^2$ .

The procedure, sketched here, is used very successfully in very many calculations for nuclear reactions, especially on light nuclei where the level density is small. The ingredients  $\gamma_{kc}^R$ ,  $E_k^0$ ,  $\Gamma_k^R$  from  $R$  matrix calculations are installed into the  $S$  matrix for nuclear reactions the standard view of which is

$$S_{cc'} = 1 - i \sum_k \frac{\gamma_{kc}^R \gamma_{kc'}^R}{E - E_k^0 + \frac{i}{2} \Gamma_k^R} \quad (1)$$

(up to a phase factor and the direct reaction part). The values  $\gamma_{kc}^R$ ,  $E_k^0$ ,  $\Gamma_k^R$  are, by definition, energy independent parameters [2].

The shortcomings of this standard  $R$  matrix calculations are the following: there is no feedback from the continuum onto the nuclear structure, the influence of decay thresholds is taken into account only by some correction terms introduced in the  $S$  matrix, and the interaction of the resonance states via the continuum is not considered. These shortcomings are important, respectively, near decay thresholds and at high level density where the resonance states overlap.

In the following, we sketch the formalism of the unified description of nuclear structure and nuclear reaction aspects (see the recent review [3]). It provides an extended version of the  $R$  matrix theory in which the energy independent parameters  $\gamma_{kc}^R$ ,  $E_k^0$ ,  $\Gamma_k^R$  are replaced by the energy dependent functions  $\tilde{\gamma}_{kc}$ ,  $\tilde{E}_k$ ,  $\tilde{\Gamma}_k$  that can be calculated in the framework of the theory. By using these ingredients, the  $S$  matrix is able to overcome the shortcomings mentioned above. It describes consistently the cross section near decay thresholds as well as nuclear reactions in the regime of high level density where narrow resonances appear together with broad ones. A model recently developed for the description of resonance states in nuclei is the Shell model embedded in the continuum [4].

### 2. The effective Hamiltonian in the subspace of discrete states

In deriving the solution of the Schrödinger equation in the whole function space, we follow Feshbach [5]. Let be  $H^{\text{full}}$  the Hamiltonian defined in the full function space with discrete as well as continuous wave functions. Then the Schrödinger equation reads

$$(H^{\text{full}} - E)\Psi_E^c = 0; \quad H^{\text{full}} = H_{QQ} + H_{QP} + H_{PQ} + H_{PP} \quad (2)$$

and  $H^{\text{full}}$  is Hermitian. We define two projection operators:

$$Q = \sum_k |\Phi_k^0\rangle\langle\Phi_k^0|; \quad (H_{QQ} - E_k^0)\Phi_k^0 = 0 \quad (3)$$

projects onto the subspace of discrete states [interior of the nucleus:  $H_{QQ} = (H_0 + V)_{QQ}$ ], and

$$P = \sum_c \int_{\epsilon_c}^{\epsilon'_c} dE |\xi_E^{c(+)}\rangle\langle\xi_E^{c(+)}|; \quad (H_{PP} - E)\xi_E^{c(+)} = 0 \quad (4)$$

projects onto the subspace of scattering states [continuum:  $H_{PP} = (H_0 + V)_{PP}$ ]. The coupling matrix elements between the two subspaces are

$$\gamma_{kc}^0 = \sqrt{2\pi} \langle\Phi_k^0|H_{QP}|\xi_E^{c(+)}\rangle. \quad (5)$$

The assumption  $Q + P = 1$  means that the  $\Psi_E^c$  contain everything.

After rewriting (2), one gets an effective Hamiltonian in the  $Q$  subspace,

$$\mathcal{H} = H_{QQ} + H_{QP}G_P^{(+)}H_{PQ}, \quad (6)$$

that is non-Hermitian. Its eigenvalues and eigenfunctions are complex,  $\mathcal{H}\tilde{\Phi}_k = \tilde{\mathcal{E}}_k\tilde{\Phi}_k \equiv (\tilde{E}_k - \frac{i}{2}\tilde{\Gamma}_k)\tilde{\Phi}_k$ , for details see the recent review [3]. The matrix elements of  $\mathcal{H}$  are

$$\begin{aligned} \langle\Phi_k^0|\mathcal{H}|\Phi_l^0\rangle &= \langle\Phi_k^0|H_{QQ}|\Phi_l^0\rangle + W_{kl}, \\ W_{kl} &\equiv \sum_{c=1}^A \mathcal{P} \int_{\epsilon_c}^{\infty} dE' \frac{\gamma_{kc}^0\gamma_{lc}^0}{E - E'} - \frac{i}{2} \sum_{c=1}^A \gamma_{kc}^0\gamma_{lc}^0 \end{aligned} \quad (7)$$

with the coupling matrix elements  $\gamma_{kc}^0$  between discrete states and scattering states. One may call  $W$  the *external interaction* appearing additionally to the *internal interaction*  $V$  involved in  $H_{QQ} = (H_0 + V)_{QQ}$ . The internal

interaction is real while the external one is complex. Since  $\gamma_{kc}^0 \gamma_{lc}^0$  is real, we have :

$$\text{Re} \{ \langle \Phi_k^0 | \mathcal{H} | \Phi_l^0 \rangle \} = \langle \Phi_k^0 | H_{QQ} | \Phi_l^0 \rangle + \sum_{c=1}^A \mathcal{P} \int_{\epsilon_c}^{\infty} dE' \frac{\gamma_{kc}^0 \gamma_{lc}^0}{E - E'}, \quad (8)$$

and

$$\text{Im} \{ \langle \Phi_k^0 | \mathcal{H} | \Phi_l^0 \rangle \} = \text{Im} (W_{kl}) = -\frac{1}{2} \sum_{c=1}^A \gamma_{kc}^0 \gamma_{lc}^0. \quad (9)$$

The principal value integral in  $\text{Re} (W_{kl})$  (second part of the rhs of Eq. (8)) does not vanish, in general. It creates energy shifts of the states, while  $\text{Im} (W_{kl})$  in Eq. (9) is related to the widths of the states.

The wave functions of the resonance states,  $\tilde{\Omega}_k = (1 + G_P^{(+)} H_{PQ}) \tilde{\Phi}_k$ , are related to the eigenfunctions of  $\mathcal{H}$ , while the energies  $\tilde{E}_k$  and widths  $\tilde{\Gamma}_k$  of the resonance states are given by the eigenvalues  $\tilde{\mathcal{E}}_k$ , see Section 3. The coupling matrix elements between resonance states and continuum are

$$\tilde{\gamma}_{kc} = \sqrt{2\pi} \langle \tilde{\Phi}_k^* | H_{QP} | \chi_E^c \rangle = \sqrt{2\pi} \langle \tilde{\Omega}_k^* | H_{QP} | \chi_E^c \rangle. \quad (10)$$

The  $\tilde{\Phi}_k$ ,  $\tilde{E}_k$ ,  $\tilde{\Gamma}_k$  and  $\tilde{\gamma}_{kc}$  are energy dependent functions that differ from the spectroscopic values (parameters):  $\tilde{\Phi}_k \neq \Phi_k^0$ ;  $\tilde{E}_k \neq E_k^0$ ;  $\tilde{\gamma}_{kc} \neq \gamma_{kc}^0$ ;  $\tilde{\Gamma}_k \leq \sum_c |\tilde{\gamma}_{kc}|^2$ . Using (6) to (10), the expression for the total wave function  $\Psi_E^c$ , that is solution of (2), as well as the  $S$  matrix can be derived,

$$S_{cc'} = 1 - i \sum_{k=1}^N \frac{\tilde{\gamma}_{kc'} \tilde{\gamma}_{kc}}{E - \tilde{E}_k + \frac{i}{2} \tilde{\Gamma}_k} \quad (11)$$

(up to a phase factor and the direct reaction part) [3]. Equation (11) coincides formally with (1). The spectroscopic ingredients are, however, different from one another in the two cases.

The basic property of a non-Hermitian operator is that its left and right eigenfunctions,  $\tilde{\Phi}_k^{\text{lt}}$  and  $\tilde{\Phi}_k^{\text{rt}}$ , are different from one another. Since the Hamiltonian  $\mathcal{H}$  is symmetric, it is  $\langle \tilde{\Phi}_k^* | \mathcal{H} = \langle \tilde{\Phi}_k^* | \tilde{\mathcal{E}}_k$  and  $\mathcal{H} | \tilde{\Phi}_k \rangle = \tilde{\mathcal{E}}_k | \tilde{\Phi}_k \rangle$ , and therefore  $\tilde{\Phi}_k^{\text{lt}} = \tilde{\Phi}_k^{\text{rt}*} \equiv \tilde{\Phi}_k^*$ . The eigenfunctions of  $\mathcal{H}$  can be orthonormalized according to

$$\langle \tilde{\Phi}_k^{\text{lt}} | \tilde{\Phi}_l^{\text{rt}} \rangle = \langle \tilde{\Phi}_k^* | \tilde{\Phi}_l \rangle = \delta_{kl} \quad (12)$$

with the consequence that

$$A_k \equiv \langle \tilde{\Phi}_k | \tilde{\Phi}_k \rangle \geq 1; \quad B_l^{l \neq k} \equiv |\langle \tilde{\Phi}_k | \tilde{\Phi}_{l \neq k} \rangle| \geq 0, \quad (13)$$

where  $\langle \tilde{\Phi}_k | \tilde{\Phi}_k \rangle = \text{Re} (\langle \tilde{\Phi}_k | \tilde{\Phi}_k \rangle)$ ;  $\langle \tilde{\Phi}_k | \tilde{\Phi}_{l \neq k} \rangle = i \text{Im} (\langle \tilde{\Phi}_k | \tilde{\Phi}_{l \neq k} \rangle) = -\langle \tilde{\Phi}_{l \neq k} | \tilde{\Phi}_k \rangle$ . The orthonormalization relations (12) hold true also at a branch point in the complex plane where two eigenvalues  $\tilde{\mathcal{E}}_k$  and  $\tilde{\mathcal{E}}_{l \neq k}$  of the effective Hamiltonian coalesce. Here, the bi-orthogonality relations (13) read  $|\langle \tilde{\Phi}_k | \tilde{\Phi}_k \rangle| \rightarrow \infty$  and  $|\langle \tilde{\Phi}_k | \tilde{\Phi}_{l \neq k} \rangle| \rightarrow \infty$ . Furthermore  $\tilde{\Phi}_k \rightarrow \pm i \tilde{\Phi}_{l \neq k}$  in approaching the branch point [3, 6].

### 3. Spectroscopic information on resonance states

The non-Hermiticity of the Hamiltonian  $\mathcal{H}$ , being effective in the  $Q$  subspace, has some consequences for spectroscopic studies of resonance states. In any case, the energies  $E_k$  and widths  $\Gamma_k$  follow from the eigenvalues  $\tilde{\mathcal{E}}_k$  of  $\mathcal{H}$ , and the coupling coefficients  $\tilde{\gamma}_{kc}$  are calculated by means of its eigenfunctions  $\tilde{\Phi}_k$ . Since the  $\tilde{\mathcal{E}}_k$  are energy-dependent functions, the values  $E_k$  and  $\Gamma_k$  are defined as the solutions of the fixed-point equations, see the following equations (14) to (17).

For isolated resonance states, we have  $A_k \rightarrow 1$  and

$$E_k = \tilde{E}_k(E = E_k) \approx E_k^0. \tag{14}$$

The widths and their relation to the partial widths are

$$\begin{aligned} \Gamma_k &= \tilde{\Gamma}_k(E = E_k), \\ \tilde{\Gamma}_k &= \frac{\sum_c |\tilde{\gamma}_{kc}|^2}{A_i} \approx \sum_c |\tilde{\gamma}_{kc}|^2 \approx \sum_c |\gamma_{kc}^0|^2 \approx \sum_c |\gamma_{kc}^R|^2 = \Gamma_k^R. \end{aligned} \tag{15}$$

These relations agree with the standard ones.

For overlapping resonance states, it is  $A_k > 1$  and

$$E_k = \tilde{E}_k(E = E_k) = E_k^0 + \Delta E_k. \tag{16}$$

The shifts  $\Delta E_k$  are usually different from zero. The widths are

$$\Gamma_k = \tilde{\Gamma}_k(E = E_k), \tag{17}$$

and the partial widths lose their physical meaning,

$$\tilde{\Gamma}_k = \frac{\sum_c |\tilde{\gamma}_{kc}|^2}{A_k} \leq \sum_c |\tilde{\gamma}_{kc}|^2. \tag{18}$$

The relations (16) to (18) show the differences to the standard relations at high level density. They can be obtained quantitatively in numerical studies.

Let us now write the Hamiltonian (6) as

$$\mathcal{H} = \mathcal{H}' - i\pi \tilde{V}^\dagger \tilde{V}; \quad \mathcal{H}' = H_{QQ} + \text{Re}\{H_{QP}G_P^{(+)}H_{PQ}\} \tag{19}$$

compare Eq. (8). Then, we have the following scenarios.

- (i) Small imaginary part of the coupling strength between system and channels: most important part of  $\mathcal{H}$  is  $\mathcal{H}'$  that is a matrix of rank  $N$  (number of states). The interaction between every two states contains the internal interaction  $V$  (contained in  $H_{QQ}$ ) and the real part of the coupling via the continuum. It is considered mostly as an effective residual interaction.
- (ii) Large imaginary part of the coupling strength between system and channels: the states of the system are strongly changed by the coupling to the channels. They can no longer be described by an effective real interaction strength in the Hamiltonian. Most important part of  $\mathcal{H}$  is  $\tilde{V}^\dagger \tilde{V}$  that is a matrix of rank  $K$  (number of open decay channels).
- (iii) Intermediate coupling regime: with increasing coupling strength between system and channels,  $N-K$  resonance states decouple from the channels while a few of them ( $K$ ) align with the  $K$  decay channels. The transition between the two limiting cases (i) and (ii) depends strongly on the individual values of the coupling matrix elements  $\tilde{\gamma}_{kc}$  according to (19).

Thus in the  $S$  matrix formalism with use of the effective Hamiltonian  $\mathcal{H}$ , the resonance states are characterized by the energy dependent eigenvalues  $\tilde{E}_k$  and eigenfunctions  $\tilde{\Phi}_k$  of the effective Hamiltonian  $\mathcal{H}$ . Furthermore, the spectroscopic values  $E_k$  and  $\Gamma_k$  are clearly defined since the effective Hamiltonian  $\mathcal{H}$  describes the open quantum system in a unique manner.

In the  $S$  matrix theory, the spectroscopic values of a resonance state are defined usually by means of the poles of the  $S$  matrix. This (standard) definition of the spectroscopic values from reactions is not a direct one since the poles of the  $S$  matrix give information on the resonances, but not on the spectroscopic properties of the resonance states. The  $S$  matrix has a pole only when the energy is continued into the complex plane. One should remind however that the  $S$  matrix describing physical processes is defined for real energies  $E$ , and  $|S|^2 \leq 1$ . It is not surprising therefore that the two definitions (by using, respectively, the effective Hamiltonian and the poles of the  $S$  matrix) do not coincide completely.

It may happen that  $E_k = E_l$  and  $\Gamma_k = \Gamma_l$  for two different states  $k$  and  $l$ , *i.e.* that two eigenvalues coalesce at a certain point in the complex plane. Such a point is a branch point in the complex plane [7,8]. It might be considered as the analogue of a double pole of the  $S$  matrix. However, the coalescence of two eigenvalues at  $E = E_k = E_l$  does not mean that also the poles exactly coalesce. This shows once more that poles and double poles of the  $S$  matrix characterize the spectroscopic values of resonance states only approximately. Using the formalism of the effective Hamiltonian with its

eigenvalues and eigenfunctions, redundantizes the search for the poles of the *S* matrix.

This statement corresponds fully to the idea of the *R* matrix theory. However, the corrections arising from the coupling of the states via the continuum have to be taken into account in a straightforward manner. They cannot be neglected in the neighbourhood of decay thresholds and at high level density. In any case the *S* matrix is, at a certain energy *E*, determined by  $\tilde{E}_k(E)$  and  $\tilde{\Gamma}_k(E)$  as well as by the eigenfunctions  $\tilde{\Phi}_k(E)$  by means of which the coupling matrix elements  $\tilde{\gamma}_{kc}(E)$  are calculated according to (10). The  $\tilde{E}_k(E)$ ,  $\tilde{\Gamma}_k(E)$  and  $\tilde{\gamma}_{kc}(E)$  at a certain energy *E* may be very different from the values  $E_k$ ,  $\Gamma_k$  and  $\tilde{\gamma}_{kc}(E_k)$ .

#### 4. Level repulsion and level attraction: some examples

It is difficult (or impossible) to trace the eigenvalues of the effective Hamiltonian  $\mathcal{H}$  for the open nuclear system in present experiments as a function of an external parameter. Moreover, the residual interaction between nucleons in nuclei cannot be derived from first principles for realistic nuclei. In theory, one is therefore obliged to work with parameters. These parameters are obtained by a fit to many different nuclear states. Practically,  $\mathcal{H}'$  in (19) is fitted but not  $\mathcal{H}$ . The description received in such a manner gives reliable spectroscopic information for stable nuclei and for nuclear states at low level density.

The situation for other open quantum systems is better than for nuclei in the sense that the interaction between the substituents of the system is smaller so that the behaviour of the resonance states can be controlled by means of external parameters. In the following, a few examples for physical effects will be shown. They will illustrate the influence of the correction term in  $\mathcal{H}$  onto the spectroscopic information that can be obtained by analyzing experimental reaction data. The results will give some hint for the analogue situation in nuclei since most of the corrections are generic [3].

Level repulsion is a phenomenon well known in the spectroscopy of discrete states. It appears also in the spectroscopy of resonance states [8]. Here, it is caused by the real part of the interaction, Eq. (8), between every two states. The imaginary part of the interaction via the continuum, Eq. (9), causes level attraction that is seldom discussed in theoretical studies. The interplay between level repulsion and level attraction is a characteristic feature of the spectroscopic properties of resonance states. It causes the phenomenon of resonance trapping [9], *i.e.* the decoupling of some resonance states from the continuum of decay channels at strong coupling strength. This phenomenon appears in different quantum systems at high level density, *e.g.*, in atoms [10], molecules [11], quantum dots [6, 12].

For illustration, in Fig. 1 [13] the motion of the eigenvalues of a rectangular quantum billiard is shown by varying the degree of coupling strength to an attached lead. The picture shows the sensitivity of the position of the eigenvalues and of the trapping process to a variation of the shape  $x_r \times y_d$  of the billiard: the length  $y_d$  is only slightly larger in the left part of the figure than in the right one.

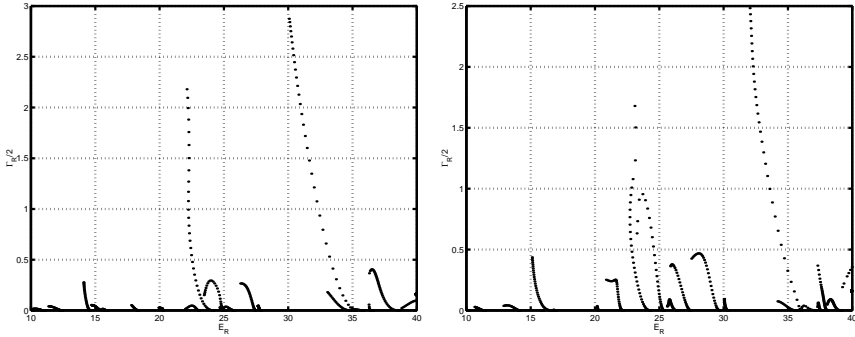


Fig. 1. Eigenvalue picture: motion of the eigenvalues of the effective Hamiltonian (solutions of the fixed-point equations) of a rectangular  $x_r \times y_d$  quantum billiard with an attached lead in dependence on increasing opening ( $w = 0.4 : 0.01 : 0$ ) for  $x_r = 1.5$ ,  $y_d = 3.34$  (left) and  $y_d = 3.28$  (right).  $x_r$ ,  $y_d$  and  $w$  are given in units of maximum opening  $1 - w = 1$  [13].

Another example is the eigenvalue picture for two atomic states under the influence of the coupling to a laser field (Fig. 2) [10]. Level repulsion occurs when  $\Omega_R \gg \Omega_c$ , and level attraction when  $\Omega_R \ll \Omega_c$  (where  $\Omega_R$  and  $\Omega_i$  are the real and imaginary parts of the Rabi frequency). The motion of the eigenvalues reflects itself in the corresponding photoionization cross sections in the vicinity of the autoionizing state 2 as a function of the probe field frequency: a narrow structure can be seen in the cross section when  $\Omega_R \ll \Omega_c$  while two separated structures appear due to level repulsion when  $\Omega_R \gg \Omega_c$  [10].

When  $Q = 0$ , laser induced degenerate states appear at a certain critical value  $I_{cr}$  of the laser intensity. At this laser intensity, two eigenvalues of the effective Hamiltonian coalesce. The corresponding point in the complex plane is a branch point. It separates the region with avoided level crossing in the complex plane from that without any crossing [6, 8].

Moreover, due to the resonance trapping phenomenon, collective modes can be generated in open quantum systems. An example are the whispering gallery modes that emerge in, *e.g.*, quantum billiards with convex shape when the leads are attached in a suitable manner [14]. The trapped states are well described by random matrix theory while the collective ones are regular modes [15].

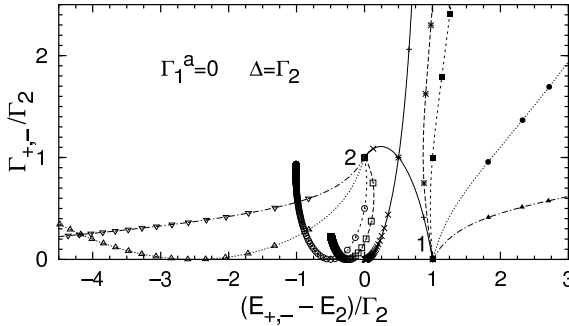


Fig. 2. The trajectories of the complex energies  $\mathcal{E}_{\pm} = E_{\pm} - \frac{i}{2}\Gamma_{\pm}$  of the states 1 and 2, obtained by varying the strong field intensity. Full line:  $Q = 0$ , broken:  $Q = 0.5$ , dashed:  $Q = 1$ , dotted:  $Q = 5$ , and chain:  $Q = 25$ . Strong field frequency detuning  $\Delta = \Gamma_2$ . Every value of  $\mathcal{E}_{\pm}$  corresponding to a variation of the intensity in steps of  $\gamma_1\Delta I = 0.5\Gamma_2$  (for  $Q = 0, 0.5, 1$ ), in steps of  $\gamma_1\Delta I = 0.25\Gamma_2$  for  $Q = 5$ , and in steps of  $\gamma_1\Delta I = 0.01\Gamma_2$  for  $Q = 25$  is marked by a symbol. The density of the symbols indicates the velocity with which  $\mathcal{E}_{\pm}$  moves as a function of  $I$  [10].

Resonance trapping has been proven directly by analyzing experimental data obtained from a quantum billiard to which a lead has been attached. The eigenvalue pictures as a function of the degree of opening to the lead show clearly the resonance trapping phenomenon [16]. In nuclear physics, resonance trapping cannot be proven directly since a control of the nucleus by means of an external parameter is, at least today, impossible. Nevertheless, hints exist. An example is the careful analysis of different reaction data on nuclei of the  $2s - 1d$  shell. The experimentalists drew the conclusion from this analysis that the interplay of various reaction time scales cannot be neglected [17].

Another interesting effect that can be seen in Fig. 2, is the appearance of population trapping defined by  $\Gamma_- = 0$  since it occurs at a finite value of the intensity  $I$  of the laser field. Population trapping can be seen as a zero in the cross section at the energy of the state 2: although the level is populated, it does not decay due to  $\Gamma_- = 0$ . Fig. 2 nicely illustrates that population trapping is caused by the interplay between direct (internal) mixing of the two states and their mixing via the continuum (external mixing). Resonance states with vanishing decay width appear also in quantum dots [6].

Thus, zeros in the cross section may appear not only due to interferences between resonance states and background, but also as a consequence of the resonance trapping phenomenon. The first case is the well-known interference zero of Fano resonances, while the second case follows from the interplay between internal and external mixing of resonance states as shown above. For further details see [10, 18].

The results discussed above remain true also when the quantum system is embedded in more than one continuum. An example is the transmission through quantum dots with, at least, two different continua. Also in such a case, resonance trapping is observed [12]. Even resonance states with vanishing decay width appear [6]. Surface effects can be seen best in double quantum dots that consist of two single dots coupled by an internal wire of length  $L$  [6]. The coupling matrix elements between double dot and leads contain the wave functions at the surface of the double quantum dot system [12]. Transmission zeros appear at energies that are determined by the spectroscopic properties of the single quantum dots. An example is shown in Fig. 3. The transmission zero at  $E = 5/12$  is a sharp dip in a region with maximum transmission. This surface effect is a third source for zeros in the cross section. For details see [6].

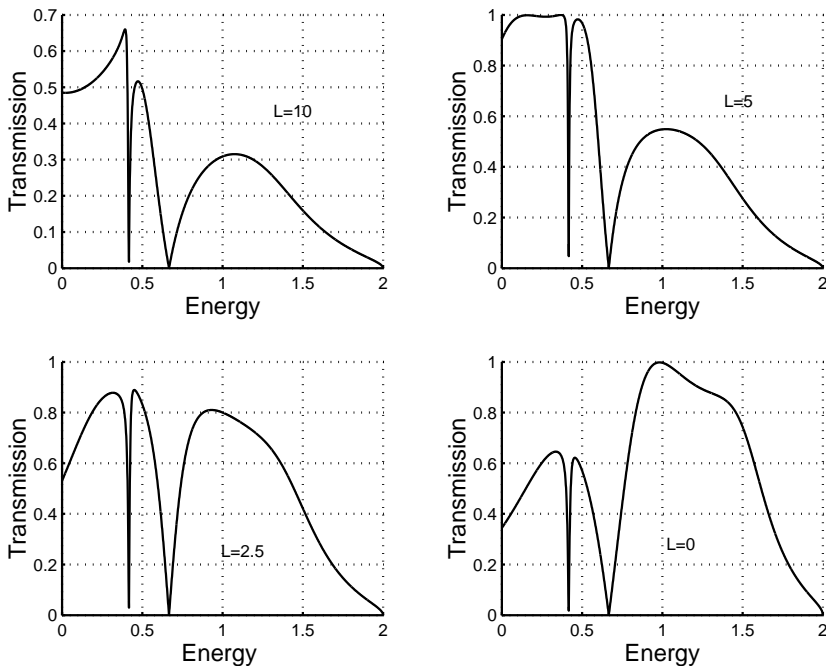


Fig. 3. Transmission through a double quantum dot. The coupling strengths of the single dots to the internal wire are  $t = 0.25$  and those to the external leads are  $v = 0.5$ . The energies of the right and left single dots are  $E_1^r = 1/3$ ,  $E_2^r = 1$ ,  $E_1^l = 1/3$ ,  $E_2^l = 1/2$ . The length of the internal wire is  $L$ . The positions of the eigenvalues of the double quantum dot depend on  $L$  while the transmission zeros are at  $E_0^r = 2/3$  and  $E_0^l = 5/12$  for all  $L$ . The mode inside the wire moves according to  $E = 1 - L/8$ .

In the calculations for quantum dots the  $P$  subspace consists of two or even more parts with  $V_{P_k P_l \neq k} = 0$ . This is, maybe, an important analogue to the problems arising in calculations for nuclei with low-lying  $\alpha$  decay thresholds. It means that there can be, *e.g.*, a subspace for nucleon channels and another one for  $\alpha$  particle channels which are coupled only via the  $Q$  subspace [19]. Furthermore, the coupling matrix elements  $V_{QP}$  and  $V_{PQ}$  embody surface effects. This property, characteristic of the  $R$  matrix theory, is important especially for systems without spherical symmetry, as has been shown by means of numerical results for double quantum dots.

These (and other) examples show that the resonance trapping phenomenon is a generic property of resonance states at high level density. It can be seen in all open quantum systems. In contrast to this result, it is assumed usually in the standard  $R$  matrix theory, that the levels broaden uniformly when the coupling strength of the system to the continuum is enlarged. Under such an assumption, different time scales will not be formed by opening the quantum system.

Level broadening is determined by the non-diagonal coupling matrix elements  $W_{kl}$  of the effective Hamiltonian  $\mathcal{H}$ , Eqs. (7) to (9). Since they are different from one another for the different states  $k, l$ , uniform level broadening can happen under special conditions only. The general scenario is resonance trapping corresponding to non-uniform level broadening,  $\sum_{k=1}^N \tilde{\Gamma}_k(a) \approx \sum_{k=1}^M \tilde{\Gamma}_k(a)$ ;  $\sum_{k=M+1}^N \tilde{\Gamma}_k(a) \approx 0$ . In the cross section, level repulsion as well as level attraction occur. Level repulsion is considered usually in the standard  $R$  matrix theory by means of the effective Hamiltonian  $\mathcal{H}'$ , Eq. (19), while level attraction is not involved in it.

## 5. Summary

Summarizing, it can be stated the following.

- (i) The effective Hamiltonian  $\mathcal{H}$  reflects the spectral properties of the closed system as well as the coupling to the environment. In the overlapping regime, complex non-diagonal matrix elements of  $\mathcal{H}$  arise from the interaction of the different resonance states via the continuum.
- (ii) The eigenvalues of  $\mathcal{H}$  determine, to a great deal, the resonance features of reactions. They are complex and energy dependent. The positions of the resonance states are shifted, generally, relative to those of the (discrete) states of the closed system. The widths of all states increase with increasing coupling strength to the continuum only at small coupling strength. At large coupling strength, however, the level broadening takes place non-uniformly: the widths of most states decrease with increasing coupling strength to the continuum while only a few ones increase.

(iii) The coupling matrix elements  $\tilde{\gamma}_{kc}$  in the pole representation (11) of the  $S$  matrix are calculated by means of the eigenfunctions of  $\mathcal{H}$  and those of the environment, see Eqs. (10) and (11). They are, as a rule, energy dependent and differ from the  $\gamma_{kc}^0$ , Eq. (5), calculated in the standard  $R$  matrix theory by means of the eigenfunctions of  $H_{QQ}$ . The sum  $\sum_c \tilde{\gamma}_{kc}$  is, generally, different from  $\tilde{\Gamma}_k$  due to the biorthogonality of the eigenfunctions of  $\mathcal{H}$ :  $\tilde{\Gamma}_k \leq \sum_c \tilde{\gamma}_{kc}$ .

The results show that an extended version of the  $R$  matrix theory can be obtained by replacing the Hermitian Hamiltonian  $H_{QQ} = (H_0 + V)_{QQ}$  (or the effective Hermitian Hamiltonian  $\mathcal{H}'$ ) by the non-Hermitian Hamiltonian

$$\mathcal{H} = (H_0 + V)_{QQ} + V_{QP} G_P^{(+)} V_{PQ} = \mathcal{H}' + \text{Im}\{V_{QP} G_P^{(+)} V_{PQ}\},$$

see Eqs. (7) up to (9) and (19). The part  $V_{QP} G_P^{(+)} V_{PQ}$  of  $\mathcal{H}$  (above all its non-Hermitian part  $\text{Im}\{V_{QP} G_P^{(+)} V_{PQ}\}$ ) contains the feedback from the continuum of decay channels onto the nuclear structure. With a small imaginary part of the coupling strength to the continuum,  $\mathcal{H} \approx \mathcal{H}'$ , one gets the standard  $R$  matrix theory with the effective Hermitian Hamiltonian  $\mathcal{H}'$  (or sometimes even the original Hermitian Hamiltonian  $H_{QQ}$ ). This means: the extended version of the  $R$  matrix theory is a natural further development of the standard  $R$  matrix theory. The imaginary part of the coupling to the continuum causes, however, physically new results such as resonance trapping. This phenomenon occurs in atoms, molecules, quantum dots, nuclei and other open quantum systems.

## REFERENCES

- [1] A.M. Lane, R.G. Thomas, *Rev. Mod. Phys.* **30**, 257 (1958).
- [2] V.I. Kukulin, V.M. Krasnopol'sky, J. Horáček, *Theory of Resonances*, Kluwer Academic Publishers, Dordrecht 1989.
- [3] J. Okołowicz, M. Płoszajczak, I. Rotter, *Phys. Rep.* **374**, 271 (2003).
- [4] K. Bennaceur, F. Nowacki, J. Okołowicz, M. Płoszajczak, *J. Phys. G* **24**, 1631 (1998); *Nucl. Phys.* **A651**, 289 (1999).
- [5] H. Feshbach, *Ann. Phys. (NY)* **5**, 357 (1958) and **19**, 287 (1962).
- [6] I. Rotter, A.F. Sadreev, to be published.
- [7] N. Moiseyev, *Phys. Rep.* **302**, 211 (1998).
- [8] I. Rotter, *Phys. Rev.* **E64**, 036213 (2001).
- [9] I. Rotter, *Rep. Prog. Phys.* **54**, 635 (1991).
- [10] A.I. Magunov, I. Rotter, S.I. Strakhova, *J. Phys.* **B32**, 1669 (1999) and **34**, 29 (2001).

- [11] M. Desouter-Lecomte, X. Chapuisat, *Phys. Chem. Ch. Ph.* **1**, 2635 (1999).
- [12] A.F. Sadreev, I. Rotter, *J. Phys. A: Math. Gen.* **36**, 11413 (2003).
- [13] I. Rotter, E. Persson, K. Pichugin, P. Šeba, *Phys. Rev.* **E62**, 450 (2000).
- [14] R.G. Nazmitdinov, K.N. Pichugin, I. Rotter, P. Šeba, *Phys. Rev.* **E64**, 056214 (2001); *Phys. Rev.* **B66**, 085322 (2002).
- [15] R.G. Nazmitdinov, H.S. Sim, H. Schomerus, I. Rotter, *Phys. Rev.* **B66**, 241302(R) (2002).
- [16] E. Persson, I. Rotter, H.J. Stöckmann, M. Barth, *Phys. Rev. Lett.* **85**, 2478 (2000); H.J. Stöckmann, E. Persson, Y.H. Kim, M. Barth, U. Kuhl, I. Rotter, *Phys. Rev.* **E65**, 066211 (2002).
- [17] P. Braun-Munzinger, J. Barrette, *Phys. Rep.* **87**, 209 (1982).
- [18] A.I. Magunov, I. Rotter, S.I. Strakhova, *J. Phys. B (London) At. Mol. Opt. Phys.* **36**, L401 (2003); *Phys. Rev.* **B68**, 245305 (2003)
- [19] V.V. Balashov, A.N. Boyarkina, I. Rotter, *Nucl. Phys.* **59**, 414 (1964).